Biochimica et Biophysica Acta, 942 (1988) 280–294
Elsevier

BBA 74072

Properties of ion channels formed by *Staphylococcus aureus* δ-toxin

Ian R. Mellor [a], David H. Thomas [b] and Mark S.P. Sansom [a]

[a] *Department of Zoology, University of Nottingham, University Park, Nottingham and* [b] *Department of Biochemistry, University of Sheffield, Sheffield (U.K.)*

(Received 3 February 1988)

Key words: Ion channel; δ-Toxin; Delta-toxin; Single-channel recording; Membrane-active polypeptide; Polypeptide; (*S. aureus*)

The δ-toxin of *Staphylococcus aureus* has been investigated in terms of its potential to form ion channels in planar lipid bilayers formed at the tip of patch electrodes. Channel formation has been shown to occur for δ-toxin concentrations in the range 0.1 to 2.0 μM. In 0.5 M KCl, two major classes of channels were seen – 'small' with conductances of 70–100 pS, and 'large' with a conductance of approx. 450 pS. Current-voltage relationships for lipid bilayers containing several δ-toxin channels revealed both voltage-dependent and independent components to channel gating. Reversal potential measurements showed the channels to be cation selective. In the presence of 3.0 M KCl, the channel gating kinetics were complex, with multiple open and closed states. The results are interpreted in terms of a model for the channel consisting of a hexameric cluster of α-helical δ-toxin molecules.

Introduction

The δ-toxin of *Staphylococcus aureus* (Fig. 1) is an extracellular cytolytic peptide which has been demonstrated to have surface-active effects on a variety of biological membranes [1–3]. It has been purified [4], sequenced [5], and subjected to physicochemical analysis [6]. These studies revealed it to be a 26 residue peptide, molecular weight 2977, which forms tetrameric and higher aggregates in aqueous solution. More recent NMR studies [7] have been directed towards the nature of the interaction of δ-toxin with lipid bilayers. They have shown that the peptide adopts a primarily α-helical conformation in the presence of phospholipid micelles. The crystallisation of δ-

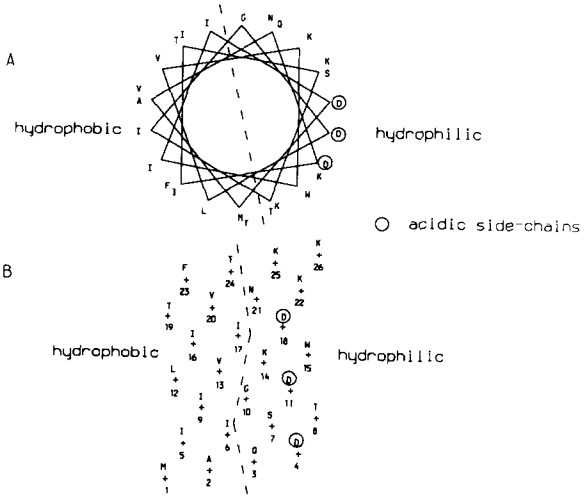

Fig. 1. α-Helical projections of the δ-toxin sequence. The amino acid sequence is viewed down (A) and parallel (B) to the axis of the α-helix. The amino acids can be seen to be partitioned between hydrophobic and hydrophilic faces of the helix. The three aspartate residues on the hydrophilic face are ringed.

Correspondence: M.S.P. Sansom, Department of Zoology, University of Nottingham, University Park, Nottingham NG7 2RD, U.K.

toxin has been reported [8], and so the availability of detailed structural information is anticipated.

We are interested in the pronounced amphipathic nature of the δ-toxin helix. Amphipathic α-helices have been investigated in attempts to relate protein and peptide structure to function [9]. Freer and Birkbeck [10] have pointed out that hexameric clusters of δ-toxin helices may form transmembrane pores, with the hydrophobic faces of the helices directed to the hydrocarbon phase of the membrane, and the hydrophilic faces forming the pore. Such a structure corresponds to the 'barrel-stave' model of the alamethicin ion channel [11], and is closely related to recent models for the channel structure of the nicotinic acetylcholine receptor [12] and other ion channels [13]. Further-more, the bee venom peptide melittin, which shares some structural similarities with δ-toxin, has been demonstrated to form ion channels in lipid bilayers [14,15]. It is therefore of interest to establish whether δ-toxin is capable of forming ion channels.

There are two main experimental configurations available for electrical recording from ion channels reconstituted into lipid bilayers [16]. Black lipid membranes [17], formed across a small hole in a Teflon film, have a relatively large area, and so a high capacitance. Improved temporal resolution during recording may be obtained by planar bilayer formation at the tip of glass microelectrodes [18], and so we elected to use the latter technique. The aims of the work described here are twofold – to demonstrate the formation of ion channels by δ-toxin, and to investigate the biophysical properties of such channels. The functional properties of the channels may then be related to the structure of the peptide molecule. A preliminary account of some of the work described here has been published in abstract form [19].

Methods

δ-Toxin was purified by the method described by Thomas et al. [8], with the following modifications. After separation on an *n*-octyl-Sepharose column, portions (approx. 2 mg) of the toxin were further purified by HPLC on an Ultrapore C_3 column (Beckman). Samples were dried under vacuum, and stored at −80 °C. Stock solutions of δ-toxin were prepared in the appropriate buffers, and also stored at −80 °C. Toxin concentrations were calculated using an absorption coefficient at 280 nm of 2.20. The lipid used for the formation of bilayers was diphytanoylphosphatidylcholine (Avanti Polar Lipids, Birmingham, AL). All other reagents were supplied by Sigma biochemicals. Unless stated otherwise, the buffer employed was 0.5 M KCl, 10 mM Bes (pH 7.0).

Pipettes were pulled from borosilicate glass (Clark Electromedical Instruments) on a Kopf model 700C puller, to give an electrode resistance, when filled with 0.5 M KCl, of approx. 10 MΩ, corresponding to a tip area of approx. 1 μm^2. Pipettes were used without further fire-polishing.

Planar bilayers were formed at the tip of the pipettes using the method of Coronado and Latorre [19]. Briefly, 15 μl of phospholipid solution (1 mg/ml in *n*-pentane) were pipetted onto the surface of 5 ml of buffer in a 10 cm^2 cross-sectional area plastic petri dish, the pipette tip having already been placed below the surface of the solution. After allowing 2 min for evaporation of the pentane, and formation of a lipid monolayer, the pipette was carefully withdrawn from the surface of the solution and replaced, thus forming a planar bilayer across the tip. The seal resistance was typically 10–100 GΩ, and the success rate for seal formation approx. 80%. The bath electrode was an Ag/AgCl electrode linked to the bath solution via an agar bridge containing 0.5 M KCl. The recording system consisted of a List EPC7 patch clamp amplifier, with the output directed to a Sony PCM linked to a standard video recorder.

The following convention is adopted with respect to membrane potential. The *cis* face of the membrane is defined as that exposed to the solution inside the pipette, and the sign of the potential is that of the *cis* face. Thus, a negative potential results in downward openings (in the figures), and a positive potential in upward openings of the channel.

All data analysis was performed using a MassComp MC5500 computer, using programs written in Fortran77 and numerical subroutines from the NAG library. Channel recordings were filtered at 1 kHz on playback, and stored on a 450 Mbyte

hard disc after analog-to-digital conversion, sampling at 5 kHz.

Histograms were constructed from the current amplitude at each sample point. For a channel with N conductance levels ($N-1$ open levels and the closed channel baseline) the current amplitude histogram was fitted by the sum of N Gaussian distributions:

$$f(i) = \sum_{j=1}^{N} P_j(\sigma_j 2\pi)^{-0.5} \exp\left[-0.5(i-g_j)^2 \sigma_j^{-2}\right]$$

where $f(i)$ is the (normalised) frequency of current amplitude i, and where P_j, g_j and σ_j are, respectively, the probability, mean and standard deviation of the jth of the N conductance levels. The fitting was carried out by non-linear least squares, using NAG subroutine E04FDF.

Single-channel records were reduced to vectors of channel dwell times using a single-threshold crossing algorithm [20]. The dwell time kinetics were analysed in terms of probability density functions (pdfs), auto-correlation functions and cross-correlation functions using methods described in previous publications from our laboratory [21–23].

Results

Formation of ion channels

Initial experiments were carried out to test the hypothesis that δ-toxin formed ion channels in bilayer membranes. A patch electrode was filled with a buffer containing 0.5 M KCl and δ-toxin. (Note that the *cis* compartment was therefore the inside of the patch electrode.) A planar bilayer was formed across the tip of the electrode and the membrane voltage clamped at, −100 mV. Current flowing through the membrane was monitored, ion channels revealing themselves as rectangular pulses of current. δ-Toxin was shown to lead to channel formation. The time of onset of channel activity was found to be quite variable, extending to several minutes after formation of the bilayer and imposition of the membrane potential.

Experiments were carried out over a range of δ-toxin concentrations. The results of three such experiments are shown in Fig. 2. For all three

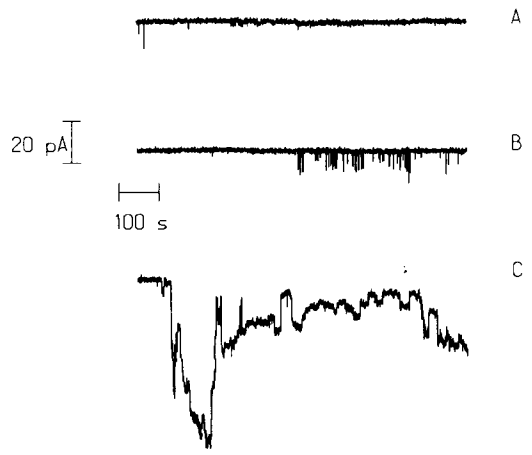

Fig. 2. Ion channel formation by δ-toxin. Three recordings are shown, made from planar bilayers held at −100 mV in the presence of δ-toxin at 0.084 (A), 0.34 (B) and 0.94 (C) μM. The electrolyte present was 0.5 M KCl.

δ-toxin concentrations a membrane potential of *cis* − 100 mV was used. The recordings shown are representative of the longest obtained in such experiments: 13.8 min for A, where 0.084 μM δ-toxin was present; 15.0 min for B, where 0.34 μM δ-toxin was present; and 19.8 min for C, where 0.94 μM δ-toxin was present.

In the presence of a low concentration of δ-toxin (A; 0.084 μM) a very low level of ion channel activity was seen. At the start of the recording, occasional brief openings of approx. 100 pS (chord conductance calculated from 10 pA current and −100 mV potential) were seen. These are somewhat obscured in Fig. 2A by the low sampling rate needed to display an extended stretch of data. Smaller openings, barely emergent form the noise level, can be seen later in the trace. Overall, the system appears to be stationary for the duration of the recording. That is, there does not seem to be an ongoing increase in the current flowing through the bilayer. It is therefore reasonable to assume that the number of δ-toxin channels in the membrane is constant, at least over the timescale of the experiment.

In the presence of a higher δ-toxin concentration (B; 0.34 μM) a higher level of channel activity was observed. However, the behaviour was stationary for over 15 min, so once again one may assume that there was no ongoing increase in the

number of δ-toxin channels formed in the membrane. Again, the details of the channel activity to be seen in Fig. 2B are suppressed by the compression of the timescale, but inspection at a higher sampling rate (see below) revealed brief channel openings of 50–100 pS (i.e. 5–10 pA).

Increasing the concentration of δ-toxin further (C; 0.94 μM) resulted in a marked increase in the level of ion channel activity. The behaviour of the system became markedly non-stationary, although there was no actual breakdown of the electrical seal for at least 20 min. Multiple conductance levels can be seen, which are likely to be due to the simultaneous presence of several δ-toxin channels within the bilayer patch. More quantitative evaluation of the number of channels and conductance levels was not possible.

Overall, it was only possible to observe formation of ion channels within a rather narrow window of δ-toxin concentrations, particularly if extended stationary recordings were required for further analysis. Below approx. 0.05 μM δ-toxin, no channel activity was detectable, even after 1 hour had elapsed since bilayer formation. At concentrations greater than approx. 2 μM, the level of activity was high and non-stationary, and rapid breakdown of the seal occurred, presumably due to lysis of the bilayer. The strong concentration dependence of channel formation must reflect a relatively large number of δ-toxin molecules needed to form a functional channel. This is analogous to the situation for alamethicin [11] and its synthetic analogues [24].

We attempted to relate the time of onset of channel activity to the concentration of δ-toxin present in the patch electrode. However the onset times were found to be extremely variable, which must reflect the stochastic nature of the underlying process of channel formation. We can therefore only state qualitatively that onset times tended to be shorter for higher δ-toxin concentrations.

The results discussed above all correspond to a membrane potential of −100 mV. However, similar results have been obtained at −50, +50 and +100 mV, over a range of δ-toxin concentrations.

Channel conductances, 'small' channels

The recording presented in Fig. 2B was analysed in more detail to obtain information about the conductance of the ion channels formed by δ-toxin.

The recording was digitized at a frequency of 5 kHz, filtering at a cutoff frequency of 1 kHz, and a current amplitude histogram constructed. In Fig. 3A a current amplitude histogram for the entirety of the recording presented in Fig. 2B is given. The large peak corresponds to the baseline current, i.e. to the closed channel. The arrow indicates the position of the (small) open channel peak, the small area of which reflects the low level of channel activity. Fitting the amplitude histogram with the sum of two Gaussian distributions gave a probability of the channel being open of $P_{o,1} = 0.012$, and a mean open channel conductance of $g_1 = 72$ pS. In Fig. 3B the same amplitude histogram is shown on a logarithmic scale. The open channel peak can be seen to be made up of a major peak and a higher conductance shoulder, as indicated by the two arrows. The histogram is a broad envelope, rather than distinct Gaussian components. This indicates that many of the channel openings were incompletely resolved at a cutoff frequency of 1 kHz, and therefore were of less than approx. 1 ms duration. Fitting the histogram with the sum of 3 Gaussian distributions gave mean conductances of $g_1 = 73$ pS and $g_2 = 101$ pS, with corresponding open probabilities of $P_{o,1} = 0.011$ and $P_{o,2} = 0.0007$. So, by consideration of the current amplitude histogram of the recording as a whole, one may conclude that the channel is open for approx. 1% of the time, that there are discrete channel conductances of $g_1 \approx 70$ pS and $g_2 \approx 100$ pS, and that there are many brief (< 1 ms) and hence incompletely resolved openings.

Channel openings were examined in more detail by selection of regions of the recording where discrete openings could be observed. An example of such is presented in Fig. 3C, with higher time resolution views of individual openings in Fig. 3D and 3E. In Fig. 3D an opening of duration approx. 0.4 s is indicated by the arrow. The amplitude histogram for the displayed data (again presented on a logarithmic scale) shows a clear open channel peak at 100 pS. Similarly, in Fig. 3E a discrete 80 pS opening is seen. These two examples are typical of numerous such openings examined. The conductances of $g_1 = 80$ pS and $g_2 = 100$ pS are in agreement with those obtained by fitting of the overall amplitude histograms.

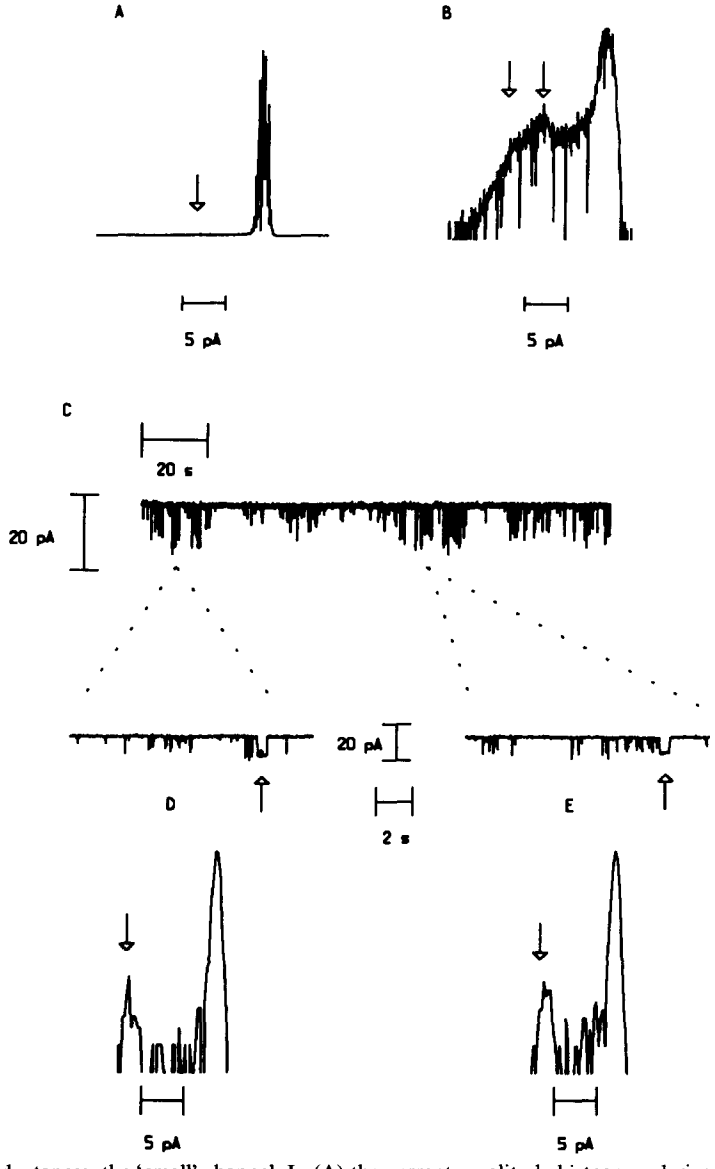

Fig. 3. δ-Toxin channel conductances, the 'small' channel. In (A) the current amplitude histogram derived from the data in Fig. 2(B) is shown. The arrow indicates the position of the (small) open channel peak. This is seen more clearly when the histogram is redrawn on a logarithmic scale (B), where the arrows indicate the positions of the two open channel conductances. In (C) an expanded section of the data is shown. Individual openings, with the corresponding current amplitude histograms (again on a logarithmic scale) below, are shown for 100 pS (D) and 80 pS (E) openings.

Conductances of $g_1 = 70–80$ pS and $g_2 = 100–110$ pS have been seen in several recordings, at different potentials, and with different δ-toxin concentrations. In addition to these levels, occassional openings of 20–30 pS are seen, although these have proved somewhat difficult to resolve unambiguously as they tend to be brief and hence bandwidth limited. Either way, such openings must contribute to the shoulder in the overall amplitude histogram between the $g_1 = 73$ pS and baseline peaks. It is tempting to identify the $g_2 = 101$ pS conductance with the sum of the two lower conductance levels, but more definitive evidence is needed to demonstrate this to be the case.

Channel conductances, 'large' channels

In addition to the 'small' channels described above, larger channel openings are also seen, particularly at higher toxin concentrations. In Fig. 4 a segment of a recording obtained in the presence of 0.34 μM δ-toxin, at a membrane potential of -100 mV, is shown, in which both 'large' and 'small' channel openings are seen.

In the lower time resolution view (A), a cluster of 'large' channel openings of duration approx. 17.5 s is seen, followed by a spell during which the channel is closed, and then a cluster of 'small' channel openings lasting for 1 min or more. Analysis of this recording via a current amplitude histogram gave a rather broad envelope, with a peak at $g_3 \approx 450$ pS corresponding to the 'large' channel openings, in addition to a shoulder at 70–100 pS.

In Fig. 4B a higher time resolution view of some of the 'large' channel openings is shown. Discrete openings, of duration approx. 200 ms, interrupted by brief closings can be seen. Current amplitude histogram analysis for this region gave conductances of 470 pS and 420 pS. Note the 'chattering' between the 470 and 420 pS levels towards the end of the openings.

In Fig. 4C a similar view is given of the 'small' channel. Again, both discrete and band-width limited events can be seen. Current amplitude histogram analysis yielded estimates of $g_1 = 75$ pS and $g_2 = 100$ pS, i.e. very close to those obtained during analysis of the 'small' channels described above.

Overall, it can be seen that δ-toxin can also lead to the formation of 'large' channels of conductance $g_3 = 450$ pS. Once again, subconductances are seen – this level appearing to be split into 420 pS and 470 pS sub-states. Such 'large' openings are very rarely seen at low (i.e. < 0.3 μM) concentrations of δ-toxin. At higher δ-toxin

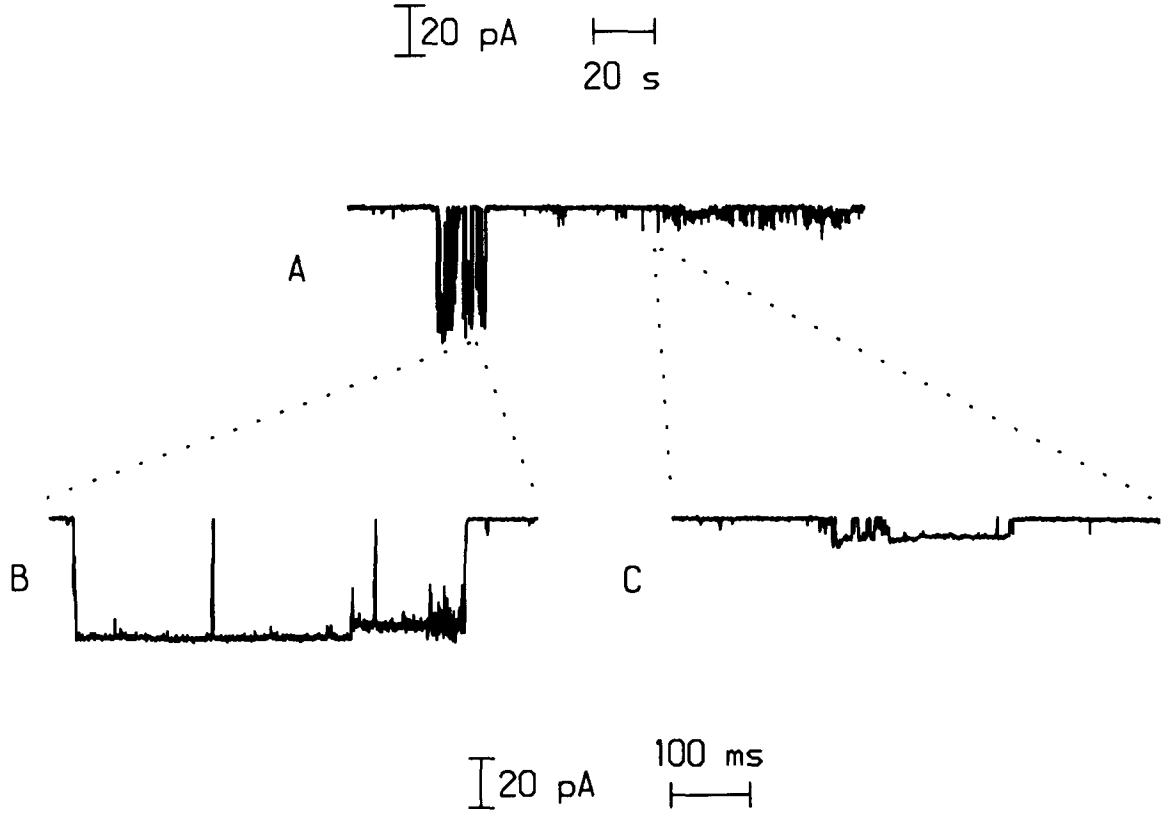

Fig. 4. δ-Toxin, 'large' channels. In (A) a segment of a recording obtained at -100 mV using 0.34 μM δ-toxin is shown. Both 'large' and 'small' conductance channels are seen, these being illustrated on an expanded timescale in (B) and (C), respectively.

concentrations such openings, and multiples thereof, are relatively common, and frequently seem to precede breakdown of the membrane seal.

Current-voltage relationships

The experiments described so far have all been conducted at a constant membrane potential. We also wished to examine the relationship between membrane potential and channel activity. To this end we formed a seal in the presence of δ-toxin, in the same manner as before, and imposed a constant potential until channel formation was initiated. Once channel openings were seen, a voltage ramp was applied, and the resultant membrane

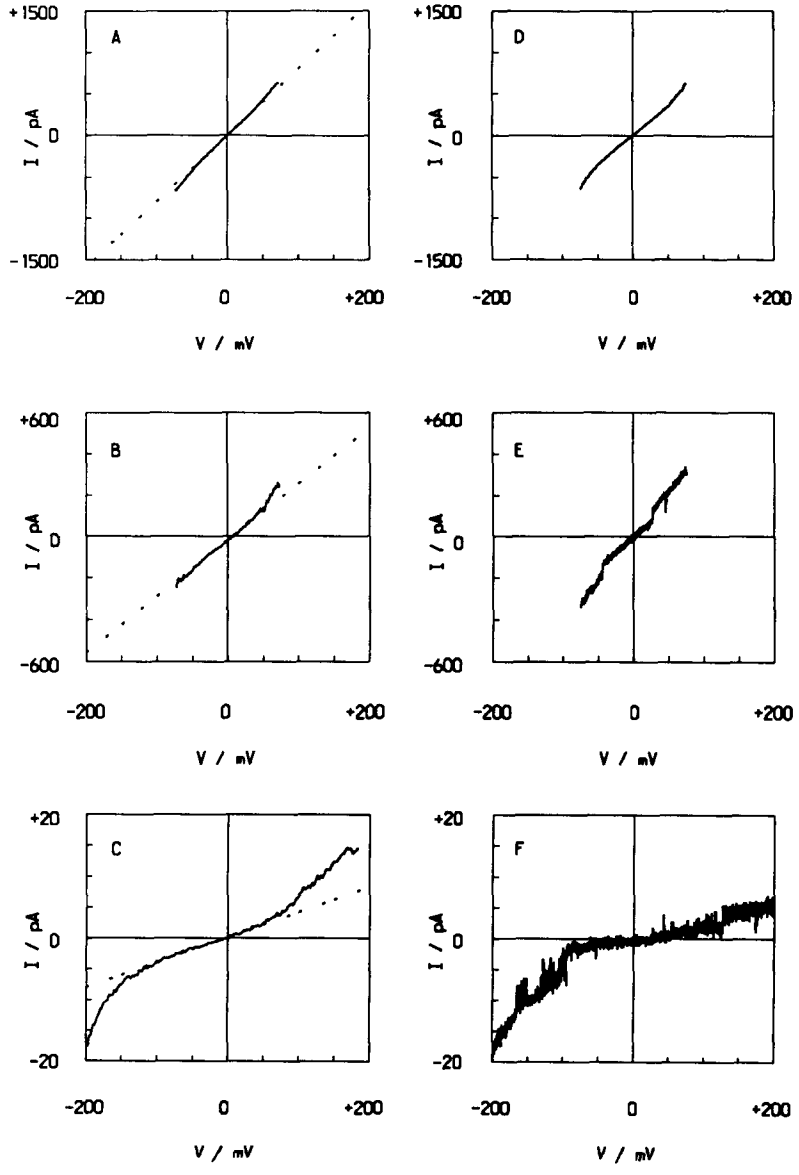

Fig. 5. Current-voltage relationships for δ-toxin. The δ-toxin concentrations are 1.88 μM (A and D), 1.24 μM (B and E) and 0.94 μM (C and F). In A, B and C the average current-voltage relationships are shown. In D, E and F the results of individual voltage-ramp experiments are given.

current measured. The voltage ramp was applied repeatedly, and the currents analysed: (a) individually, ramp by ramp, in terms of discrete transitions between conductance levels (now measured in terms of slope rather than chord conductances); and (b) by averaging the recordings from individual voltage ramps so as to obtain average current-voltage relationships.

In Fig. 5 current-voltage relationships thus obtained are shown for three concentrations of δ-toxin, namely: 1.88 μM (A and D), with a −75 to +75 mV voltage ramp; 1.24 μM (B and E), also with a −75 to +75 mV voltage ramp; and 0.94 μM (C and F), with a −200 to +200 mV voltage ramp imposed. In each case the ramp duration was 10 s. In A, B and C the average current-voltage relationships are shown, in D, E and F typical individual current responses to voltage ramps are given.

The average current-voltage relationships are approximately symmetrical about 0 mV, and deviate from linearity at potentials of greater than 60 mV in magnitude. This latter feature is most evident in C (0.94 μM δ-toxin) where it was possible to impose a voltage ramp of ±200 mV. At higher δ-toxin concentrations, attempts to impose such a voltage range generally resulted in breakdown of the membrane seal. Consequently, it was only possible to explore a narrower voltage range, and the observed deviations from linearity of the current-voltage relationships are much smaller. Non-linear current-voltage relationships are indicative of either: (a) a voltage dependent component to channel gating; and (b) non-linear single-channel current-voltage behaviour. Non-linear current-voltage curves have been reported for melittin [14] and for alamethicin and its synthetic peptide analogues [24].

Individual current-voltage curves were analysed in an attempt to determine whether the current-voltage relationships of single channels were linear or not, and also to obtain estimates of channel conductances independent from those described in the previous sections. At 1.88 μM δ-toxin (D) the individual current-voltage relationships were still smooth curves, with no discrete channel openings. The conductance at 0 mV was 6.7 nS. If one assumes this to be made up primarily of 'large' ($g_3 \approx 450$ pS) conductance channels, this would correspond to approx. 15 channels open simultaneously. As in the average curve, the relationship becomes non-linear at approx. 60 mV.

In the presence of 1.24 μM δ-toxin, discrete channel openings may be seen. Thus, in Fig. 5E, the conductances of the three regions (left to right) are 4.8 nS, 2.9 nS and 3.8 nS. The first transition would correspond to the closing of four 'large' conductance channels, and the second transition to the opening of two channels. Examination of 16 ramps in this manner revealed several conductance changes, all of which were approximate multiples of 450 pS. Note also in Fig. 5E that the current-voltage relationships for the sections between transitions are linear, and that the channels appear to open as the magnitude of the potential is increased.

In the presence of a relatively low concentration of δ-toxin (0.94 μM, F), the individual current-voltage relationships are much more noisy, with frequency switching between different conductance levels. However, clear changes in slope conductance can be seen and measured. Analysis of 16 ramps revealed three major slope conductances, at 24 ± 10 pS, 78 ± 15 pS, and 121 ± 6 pS. The latter two of these correspond well with the estimates of $g_1 = 73$ pS and $g_2 = 101$ pS obtained from chord-conductance measurements. The conductance of 24 pS may correspond to the shoulder observed between 73 pS and 0 pS in Fig. 3B, which could not be resolved when fitting the amplitude histogram.

Overall, analysis of the individual current-voltage relationships supports the idea that the non-linear average relationships result from a voltage dependent component of channel gating. At both 1.24 and 0.94 μM δ-toxin the sections of the current-voltage plots between transitions are linear, and openings to higher conductance levels occur more often at higher potentials.

We have attempted to relate the average conductance at 0 mV to the concentration of δ-toxin present. This has proved somewhat difficult, as variation between experiments occurs, with occasional failure to observe any channels, even after holding the potential at ±100 mV for extended periods of time. However, if one plots the conductances at 0 mV, for the data in Fig. 5, against δ-toxin concentration on a double logarithmic plot,

a slope of approximately 7 is obtained. This is in reasonable agreement with the proposal of Freer and Birkbeck [10] that 6 δ-toxin molecules make up the ion channel.

Ion selectivity

We have attempted to determine the cation/anion selectivity of δ-toxin channels by measurement of reversal potentials, i.e., the potentials at which there is no net flow of current, when there was a 5-fold difference in the KCl concentration between the *cis* and *trans* faces of the membrane. Reversal potentials were estimated both from voltage-ramp experiments, and by measurement of single channel amplitudes over a range of (constant) potentials.

Single-channel measurements suggested that 'small' (70–100 pS) and 'large' (450 pS) channels reversed at different potentials. For example, with *cis* 0.5 m KCl and *trans* 0.1 M KCl, 'small' channels reversed at −30 mV, whereas 'large' channels reversed at −15 mV.

The voltage ramp experiments gave an estimate of the reversal potential of 'large' channels (slope conductances of 450 to 1000 pS) of +15 mV when *cis* KCl was 0.6 M and *trans* KCl was 3 M.

It therefore seems that the 'small' channels are more cation/anion selective than the 'large' channels. Using the Goldman-Hodgkin-Katz equation the above reversal potentials give permeability ratios of $P_K/P_{Cl} = 9.3$ for the 'small' channel and $P_K/P_{Cl} = 2.6$ for the 'large' channel. Thus the 'large' channels are only weakly selective for cations over anions, whereas the 'small' channels are more markedly selective.

Channel kinetics

We were also interested in the gating kinetics of the 'small' δ-toxin channels. In 0.5 M KCl (as for the experiments in Fig. 3) it was difficult to make kinetic measurements as many channel openings were extremely brief and consequently were bandwidth limited. To overcome this difficulty, we tried increasing the KCl concentration to 3.0 M, given the observation of Hanke et al. [15] that channels formed by mellitin were more discrete when the NaCl concentration was raised from 1.0 M to 5.0 M.

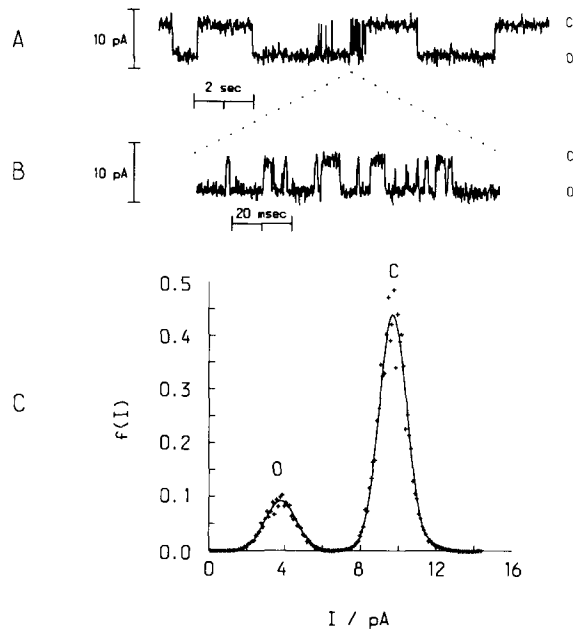

Fig. 6. δ-Toxin channels at high ionic strength. Details of data used for the kinetic analysis, obtained using 0.34 μM δ-toxin in the presence of 3.0 M KCl, at a membrane potential of −50 mV. In (A) a 13 s section of the data is shown, with C and O indicating the closed and open channel, respectively. The expanded view in (B) reveals that the majority of channel openings are fully resolved. This is confirmed by the amplitude histogram in (C), where the crosses represent the experimental data, and the curve the fitted sum of two Gaussian components, with an open channel conductance of 120 pS.

The results of such an experiment, with δ-toxin present at a concentration of 0.34 μM and a membrane potential of −50 mV, are shown in Fig. 6. This shows a 13 s section (A) from a 100 s recording in which only a single channel was present. Amplitude histogram analysis (C) of the complete recording revealed two well resolved Gaussian components, with a mean open channel conductance of 120 pS and open channel probability of $P_o = 0.20$. The higher time resolution view (B) shows that the majority of the channel openings are completely resolved. This is supported by the absence of any contribution to the amplitude histogram between the channel open and closed peaks. Hence this data was well suited to kinetic analysis of δ-toxin channel gating.

After conversion to a vector of dwell (open and closed) times, overall kinetic parameters were evaluated. The mean and standard deviation of

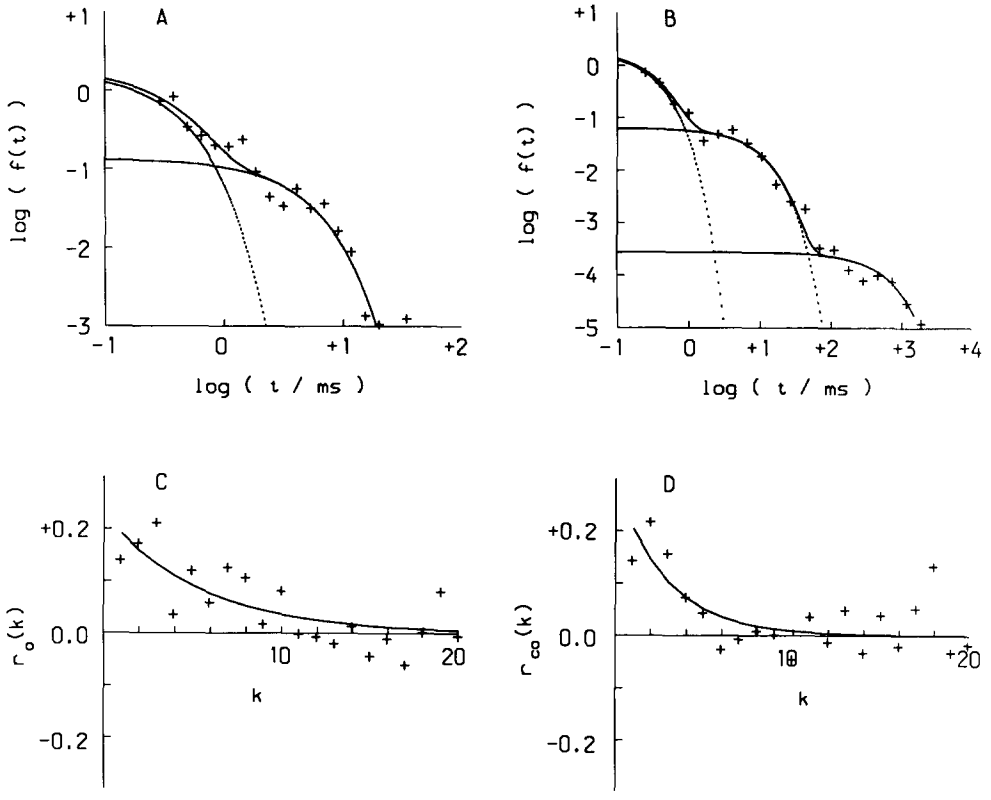

Fig. 7. Kinetic analysis of δ-toxin channel gating. In (A), the open-time histogram (crosses) and fitted pdf (solid curve) is given. The broken curve represents the two components of the fitted equation:

$$f(t) = (\alpha_1/\tau_1)\exp(-t/\tau_1) + (\alpha_2/\tau_2)\exp(-t/\tau_2)$$

where: $\alpha_1 = 0.53$ (± 0.08), $\tau_1 = 0.30$ (± 0.08) ms, $\alpha_2 = 0.52$ (± 0.11), and $\tau_2 = 3.9$ (± 1.4) ms.
In (B) the closed-time histogram and fitted pdf is presented in a similar manner. The pdf fitted is:

$$f(t) = (\alpha_1/\tau_1)\exp(-t/\tau_1) + (\alpha_2/\tau_2)\exp(-t/\tau_2) + (\alpha_3/\tau_3)\exp(-t/\tau_3)$$

where: $\alpha_1 = 0.50$ (± 0.03), $\tau_1 = 0.26$ (± 0.03) ms, $\alpha_2 = 0.55$ (± 0.08), $\tau_2 = 8.6$ (± 1.8) ms. $\alpha_3 = 0.15$ (± 0.33), and $\tau_3 = 540$ (± 1800) ms.
The open-time autocorrelation function is shown in (C) fitted by a single geometrically decaying function:

$$r_o(k) = a\pi^k$$

where $a = 0.23$ (± 0.05) and $\pi = 0.83$ (± 0.05).
The cross-correlation function, between closed times and the following open times, is given in (D), again fitted by a single geometrically decaying function:

$$r_{co}(k) = a\pi^k$$

where $a = 0.29$ (± 0.09) and $\pi = 0.71$ (± 0.09).

the channel open times were $m_o = 99.3$ ms, and $s_o = 330$ ms. For the closed times the mean and standard deviations were $m_c = 252$ ms and $s_c = 1320$ ms. These results were quite surprising. For a relatively simple molecule such as δ-toxin, we had expected that the gating process would be satisfactorily modelled by a simple gating mechanism:

$$C \underset{k_{2,1}}{\overset{k_{1,2}}{\rightleftharpoons}} O$$

for which the relevant dwell time statistics would be [25]: $m_o = k_{2,1}^{-1}$; $s_o = k_{2,1}^{-1}$; $m_c = k_{1,2}^{-1}$; and $s_c = k_{1,2}^{-1}$. That the observed dwell time standard deviations were greater than the corresponding means suggested that the dwell time probability density functions (pdfs) were sums of several exponential components, and that the underlying gating mechanism was consequently more complex than that given above.

Channel dwell time pdfs and the corresponding fits are given in Fig. 7A (open-time pdf) and 7B (closed-time pdf). The open-time pdf is described by the sum of two exponential components, with time constants $\tau_1 = 0.30$ ms and $\tau_2 = 3.9$ ms. There were also some long openings (mean duration approx. 950 ms), but these were insufficiently frequent for it to be possible to estimate the corresponding component of the pdf. We may therefore conclude that the number of open states of the gating mechanism is $N_o \geq 2$ [26].

The closed time pdf was best fitted by the sum of three exponential components. Therefore, $N_c \geq 3$. The time constants of the components were: $\tau_1 = 0.26$ ms; $\tau_2 = 8.6$ ms; and $\tau_3 = 540$ ms. Again, there were a few very long closings (mean duration approx. 8 s), but it was not possible to fit the corresponding pdf component.

Auto- and cross-correlation analyses [21–23] were also performed on the gating kinetic data. The aim of such analyses is to provide more information concerning the topology of the gating mechanism, namely whether there is a single or multiple gateway states connecting the closed states with the open. The results of such analysis are presented in Figs. 7C and 7D. The auto-correlation function is non-null (C), indicative of the minimum number of gateway states being $N_g \geq 2$. The cross-correlation function (D) is non-null and positive, indicative of long openings being paired with long closings, and short openings with short closings. This is in agreement with visual inspection of the single channel record, which shows 'gearshifting' [27] between apparent high and low frequency modes.

Discussion

δ-Toxin as a model ion channel former

One reason for studying δ-toxin is as a model for ion channels of excitable membranes, such as the nicotinic acetylcholine receptor (nAChR). The basis for this is the proposal that δ-toxin may form ion channels via formation of a cluster of transmembrane α-helices [10]. Some support for this comes from the demonstration of α-helix formation by δ-toxin in the NMR studies of Lee et al. [7].

Much of the existing work on model channels centres about the antibiotic gramicidin [28]. Whilst this has provided us with important concepts concerning the nature of ion channels, the β-helical structure adopted by gramicidin is not found in protein molecules. Interest in formation of ion channels by α-helix clusters has concentrated upon alamethicin, particularly since the structural work of Fox and Richards [29]. More recently, such models for channel formation have been adopted for the interpretation of the amino acid sequences determined for the nAChR and other channel proteins, with the proposal of detailed models by Finer-Moore and Stroud [12] and others [30]. Finally, Furois-Corbin and Pullman [31,32] have carried out detailed theoretical investigations into possible channel formation by α-helix clusters.

δ-Toxin may be compared with other α-helical channel-forming peptides. Alamethicin is probably the best understood system, especially since the work of Menestrina et al. [24] on the properties of channels formed by a range of alamethicin analogues. These peptides are all extremely hydrophobic, containing the α,α-dimethylated amino acid α-aminoisobutyric acid. δ-Toxin differs from alamethicin in that it contains only naturally occurring amino acids. In this respect it is closely related to melittin. However, unlike melittin, the amino acid sequence of δ-toxin does not contain a proline residue, the presence of which in melittin results in a pronounced bend in the helix [33]. Current structural models for the nAChR and for the voltage-gated Na^+ channel do not incorporate such a bend in the channel forming helices.

δ-Toxin is an extremely amphipathic peptide, with a clear partition of amino acid sidechains between hydrophobic and hydrophilic faces of the helix (Fig. 1). To quantify this, we have evaluated the hydrophobic moment of δ-toxin, using the method of Eisenberg [34], and the hydrophobicity indices of Kyte and Doolittle [35]. The magnitude of the mean hydrophobic moment measures the

extent of partitioning of residues between the two faces of the helix. The values arrived at are: δ-toxin 2.03; MA-helix [12] of nAChR α-subunit 1.74; and melittin 1.23. Therefore δ-toxin is highly suited to testing the nature of ion channels formed by clusters of amphipathic helices.

Formation of ion channels

Ion channel formation has been demonstrated to be optimal at δ-toxin concentrations of approx. 0.3 μM. At concentrations in excess of 2 μM loss of the electrical seal between the patch electrode and bilayer was experienced. The concentrations for channel formation are compatible with those required for the lytic activity of δ-toxin to be seen. Using calcein release to monitor lysis of gel phase dipalmitoylphosphatidylcholine vesicles, Yianni et al. [36] obtained optimal lysis in the presence of 2.3–4.6 μM δ-toxin. In these latter studies, a lag of approx. 20 s was seen before significant lysis occurred. It is possible that the nonstationary multiple channel formation followed by loss of electrical seal which we experienced in the presence of high δ-toxin concentrations reflected a similar process. This would be comparable with the proposal of Tosteson et al. [37] that haemolysis by melittin is preceded by ion channel formation.

Channel conductances

In analysing current amplitude histograms in terms of channel conductances a problem is encountered in that many channel openings are brief, relative to the filter cutoff frequency, and hence are bandwidth limited. This leads to an ambiguity [20] in that one cannot distinguish between very rapid switching between a small number of discrete channel conductance states, and the existence of a spectrum of channel conductances. The presence of peaks in the amplitude histogram, and the results obtained using 3.0 M KCl as the electrolyte lend some support to the former hypothesis. A similar problem was faced by Hanke et al. [15] in interpreting channel recordings obtained using the alamethicin analogue trichotoxin A40.

Two 'small' channel conductances, of approx. 70 and 100 pS, were identified by the above approach. These conductances are comparable to those seen for channels from excitable cell membranes, suggesting that it is not unreasonable to use simple peptides as models for the latter. For example, the reconstituted nAChR [38] has a conductance of 45 pS, and the locust muscle glutamate receptor-channel a conductance of 130 pS [39].

'Large' channels of conductance approx. 450 pS have also been seen, in both constant potential and voltage ramp experiments. We are interested in the possibility that such channels might resemble simple diffusion limited electrolyte filled pores in the bilayer. The conductance of such a pore, of length l and radius r, is given by:

$$g = \pi r^2 \rho^{-1} (l + \pi r/2)^{-1}$$

where ρ is the resistivity of the electrolyte solution [40]. We have modelled the channel as a regular hexagonal cluster of α-helices (Fig. 8), using a helix diameter of 0.86 nm [31], which gives an approximate pore radius $r = 0.43$ nm. Using a helix length of $l = 3.9$ nm, and a resistivity of $\rho = 0.13$ Ωm (calculated from tables in [41]), this gives a single channel conductance of $g = 950$ pS, i.e. approximately twice the conductance of the 'large' δ-toxin channels. This suggests that the 'large' channels indeed may be modelled, at least to a first approximation, as electrolyte filled pores.

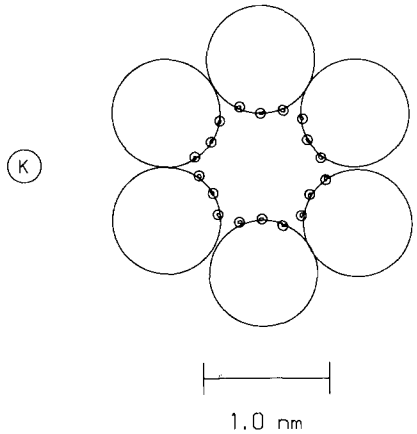

Fig. 8. Proposed structure of the δ-toxin channel. The hexameric cluster model of the δ-toxin channel is shown, viewed down the channel axis. The six large circles represent the α-helices, with the 18 small circles representing the approximate positions of the aspartate residues. A potassium ion is shown on the same scale for comparison.

The conductance levels of δ-toxin channels may be compared with those obtained in related studies. Melittin exhibits 'small' channels of conductance 5–10 pS (in 0.5 M KNO_3), alongside 'large' channels of conductance 100–2000 pS [37]. In 5.0 M NaCl, the predominant conductance was approx. 500 pS [15]. Alamethicin and its analogues show 'large' conductance channels of the order of 10 nS, the conductance being higher for the shorter analogues [24]. In all of these systems therefore, multiple conductance levels are seen. Interestingly, there has recently been some attention paid to the idea of a single receptor-channel complex showing multiple channel conductances in studies of vertebrate glutamate receptors [42,43].

Current-voltage relationships

The current-voltage relationships obtained via application of voltage ramps provide independent confirmation of the estimates of channel conductances from constant voltage experiments. More importantly, they give clues as to the nature of δ-toxin channel gating. Current-voltage relationships for δ-toxin are linear at voltages close to $V = 0$ mV, with the slope increasing with increasing δ-toxin concentration. This indicates that there is a significant voltage-independent component to channel gating, i.e. δ-toxin will form channels spontaneously in the absence of an applied potential. At membrane potentials in excess of approx. 60 mV, the current-voltage relationships become non-linear, this being more marked at low peptide concentrations. This indicates that there is also a voltage dependent component to gating. These results are qualitatively similar to those obtained with alamethicin and its analogues [24], and with melittin [14]. However, they differ quantitatively in that the voltage independent conductance seems to be more important with δ-toxin, and the degree of non-linearity is much less than in the other systems.

δ-Toxin was nominally applied to only the *cis* face of the bilayer. However, the current-voltage relationships are approximately symmetrical about $V = 0$ mV, in contrast to the situation observed for melittin [14] and for the wasp venom peptide mastoparan (Mellor and Sansom, unpublished results). Given the asymmetrical distribution of charge along the δ-toxin molecule, this implies that δ-toxin has equilibrated itself between the two faces of the bilayer after formation of the seal. Further investigations are required to confirm this proposal.

Analysis of the concentration dependence of the voltage independent conductance suggested a 7th power dependence. This is close to that predicted from the hexameric model of the δ-toxin pore (Fig. 8). We have retained the hexameric model for the present, particularly in view of the suggestion from modelling studies [31] that α-helices form irregular collapsed clusters when a heptamer is formed.

Ion selectivity

From measurements of reversal potentials, again using both constant voltage and voltage ramp experiments, we conclude that δ-toxin channels are selective for cations over anions, and that the degree of selectivity is less for the 'large' channel. This may be compared with the results for alamethicin analogues [24], for which the (small) voltage independent channels are reasonably selective, this time for anions ($P_{Cl}/P_K = 5–9$), whilst the (large) voltage dependent channels reverse at potentials close to 0 mV. Melittin has been demonstrated to be anion selective by ionic substitution experiments [14].

From examination of the hexameric cluster model of the δ-toxin channel (Fig. 8) one can arrive at a tentative explanation of the cation selectivity. If the α-helices are arranged such that their hydrophobic faces are directed away from the central pore, and their hydrophilic faces towards it, then three rings of six negatively charged aspartate residues line the channel. These would be expected to confer cation selectivity.

It is interesting that the selectivity is less for the 'large' channel. This would be consistent with this channel being close to an electrolyte filled pore in structure. There remains the question of what the structural difference between the 'large' and 'small' channels is. On the basis of the difference in selectivity, one possibility is that the helices twist about their central axes, moving the aspartate sidechains in and out of the pore, and thus modulating the conductance and ion selectivity. Structural studies will be required before this hypothesis can be further evaluated.

At this point it is informative to consider why δ-toxin channels, and those of model peptide channels in general, appear to be less ion selective than the channels of excitable cell membranes. Assuming that the latter channels are actually formed by clusters of helices, it is conceivable that the remainder of the protein molecule constrains the helices more tightly, thus making the pore less malleable to changes in the permeant ion.

Gating kinetics

Increasing the KCl concentration from 0.5 to 3.0 M appears to slow down the gating of the channel sufficiently that the majority of openings are fully resolved. The mechanism underlying this effect is not known. Studies on the physico-chemical properties of δ-toxin in aqueous solution have shown that its aggregation state is sensitive to the pH, nature and concentration of electrolytes [6]. Alternatively, it could be that increased ionic strength effects gating by decreasing the strength of electrostatic interactions within the putative electrolyte filled pore.

The results of the kinetic study provide us with constraints on the nature of the underlying gating mechanism, namely: $N_c \geq 3$; $N_o \geq 2$; and $N_g \geq 2$. Whilst these do not uniquely identify the gating mechanism, they allow one to suggest mechanisms such as:

$$\begin{array}{ccccc} C_1 & \rightleftharpoons & C_2 & \rightleftharpoons & C_3 \\ & \nwarrow\!\!\searrow & & \nwarrow\!\!\searrow & \\ & O_1 & & O_2 & \end{array}$$

in which O_1 and O_2 differ in the mean time spent open by the channel as being compatible with the observed kinetics. From the cross-correlation analysis one may state that the brief-lived open state is linked to the brief-lived closed state (O_1 to C_2, for example) and the long-lived open state to the long-lived closed state (O_2 to C_3). To relate such mechanisms to underlying molecular events will require channel kinetics to be studied as a function of membrane potential and peptide concentration. For example, we are anxious to determine whether the very long channel closings (not incorporated in the above model) correspond to disassembly of the α-helix cluster within the membrane.

Overall, we have shown that δ-toxin forms cation-selective ion channels, the gating of which is modulated by membrane potential and electrolyte concentration. Studies are underway to characterise the gating properties more fully, and to relate these properties to the molecular structure of the channel.

Acknowledgements

This work was supported by a grant from the Wellcome Trust (to M.S.P.S.). We wish to thank Dr. D. Rice (Sheffield University) for the gift of δ-toxin, and for discussions concerning its structure, and Dr. R.L. Ramsey for assistance with computing.

References

1 McCartney, A.C. and Arbuthnot, J.P. (1978) in Bacterial Toxins and Cell Membranes (Jeljaszewicz, J. and Wadstrom, T., eds.), pp. 89–127, Academic Press, London.
2 Freer, J.H., Birkbeck, T.H. and Bhakoo, M. (1984) in Bacterial Protein Toxins (Alouf, J.E., Fehrenbach, F.J., Freer, J.H. and Jeljaszewicz, J., eds.), pp. 179–189, Academic Press, London.
3 Bernheimer, A.W. and Rudy, B. (1986) Biochim. Biophys. Acta 864, 123–141.
4 Heatley, N.G. (1971) J. Gen. Microbiol. 69, 269–278.
5 Fitton, J.E., Dell, A. and Shaw, W.V. (1980) FEBS Lett. 115, 209–212.
6 Fitton, J.E. (1981) FEBS Lett. 130, 257–260.
7 Lee, K.H., Fitton, J.E. and Wuthrich, K. (1987) Biochim. Biophys. Acta 911, 144–153.
8 Thomas, D.H., Rice, D.W. and Fitton, J.E. (1986) J. Mol. Biol. 192, 675–676.
9 Kaizer, E.T. and Kezdy, F.J. (1983) Proc. Natl. Acad. Sci. USA 80, 1137–1143.
10 Freer, J.H. and Birkbeck, T.H. (1982) J. Theor. Biol. 94, 535–540.
11 Latorre, R. and Alvarez, O. (1981) Physiol. Rev. 61, 77–150.
12 Finer-Moore, J. and Stroud, R. (1984) Proc. Natl. Acad. Sci. USA 81, 155–159.
13 Barnard, E.A., Darlison, M.G. and Seeburg, P. (1987) Trends Neurosci. 10, 502–509.
14 Tosteson, M.T. and Tosteson, D.C. (1981) Biophys. J. 36, 109–116.
15 Hanke, W., Methfessel, C., Wilmsen, H.-U., Katz, E., Jung, G. and Boheim, G. (1983) Biochim. Biophys. Acta 727, 108–114.
16 Coronado, R. (1986) Annu. Rev. Biophys. Biophys. Chem. 15, 259–277.
17 Montal, M. and Mueller, P. (1972) Proc. Natl. Acad. Sci. USA 69, 3561–3566.

18 Coronado, R. and Latorre, R. (1983) Biophys. J. 43, 231–236.
19 Sansom, M.S.P. and Mellor, I.R. (1987) Neuroscience 22, S685.
20 Colquhoun, D. and Sigworth, F.J. (1983) in Single-Channel Recording (Sackmann, B. and Neher, E., eds.), pp. 191–263, Plenum Press, New York.
21 Kerry, C.J., Kits, K.S., Ramsey, R.L., Sansom, M.S.P. and Usherwood, P.N.R. (1987) Biophys. J. 51, 137–144.
22 Ball, F.G. and Sansom, M.S.P. (1988) Biophys. J. 53, 819–832.
23 Ball, F.G., Kerry, C.J., Ramsey, R.L., Sansom, M.S.P. and Usherwood, P.N.R. (1988) Biophys. J. 54, in press.
24 Menestrina, G., Voges, K.-P., Jung, G. and Boheim, G. (1986) J. Membr. Biol. 93, 111–132.
25 Colquhoun, D. and Hawkes, A.G. (1983) in Single-Channel Recording (Sakmann, B. and Neher, E., eds.), pp. 135–175, Plenum Press, New York.
26 Colquhoun, D. and Hawkes, A.G. (1981) Proc. R. Soc. Lond. (Biol.) 211, 205–235.
27 Moczydlowski, E. (1986) in Ion Channel Reconstitution (Miller, C., ed.), pp. 75–113, Plenum Press, New York.
28 Andersen, O.S. (1984) Annu. Rev. Physiol. 46, 531–548.
29 Fox, R.O. and Richards, F.M. (1982) Nature 300, 325–330.
30 Guy, H.R. and Hucho, F. (1987) Trends Neurosci. 10, 318–321.
31 Furois-Corbin, S. and Pullman, A. (1986) Biochim. Biophys. Acta 860, 165–177.
32 Furois-Corbin, S. and Pullman, A. (1987) Biochim. Biophys. Acta 902, 31–45.
33 Terwilliger, T.C. and Eisenberg, D. (1982) J. Biol. Chem. 257, 6016–6022.
34 Eisenberg, D., Schwartz, E., Komaromy, M. and Wall, R. (1984) J. Mol. Biol. 179, 105–132.
35 Kyte, J. and Doolittle, R.F. (1982) J. Mol. Biol. 157, 105–132.
36 Yianni, Y.P., Fitton, J.E. and Morgan, C.G. (1986) Biochim. Biophys. Acta 856, 91–100.
37 Tosteson, M.T., Alvarez, O. and Tosteson, D.C. (1985) Regul. Pept. 13, (Suppl. 4) 39–45.
38 Montal, M., Anholt, R. and Labarca, P. (1986) in Ion Channel Reconstitution (Miller, C., ed.), pp. 157–204, Plenum Press, New York.
39 Patlak, J.B., Gration, K.A.F. and Usherwood, P.N.R. (1979) Nature 278, 643–645.
40 Hille, B. (1984) Ionic Channels of Excitable Membranes, pp. 184–186, Sinauer, Sunderland, MA.
41 Robinson, R.A. and Stokes, R.H. (1965) Electrolyte Solutions, 571 pp., Butterworths, London.
42 Jahr, C.E. and Stevens, C.F. (1987) Nature 325, 522–525.
43 Cull-Candy, S.G. and Usowicz, M.M. (1987) Nature 325, 525–528.